IEEE Access
Multidisciplinary | Rapid Review | Open Access Journal

Received December 3, 2020, accepted December 20, 2020, date of publication December 23, 2020, date of current version January 5, 2021.

Digital Object Identifier 10.1109/ACCESS.2020.3046852

Emulation of Radio Technologies for Railways: A Tapped-Delay-Line Channel Model for Tunnels

HAO QIU[1,2], (Student Member, IEEE), JUAN MORENO GARCÍA-LOYGORRI[3,4], (Senior Member, IEEE), KE GUAN[1,2], (Senior Member, IEEE), DANPING HE[1,2], (Member, IEEE), ZIHENG XU[1,2], BO AI[1,2], (Senior Member, IEEE), AND MARION BERBINEAU[5], (Member, IEEE)

[1]State Key Laboratory of Rail Traffic Control and Safety, Beijing Jiaotong University, Beijing 100044, China
[2]Beijing Engineering Research Center of High-speed Railway Broadband Mobile Communications, Beijing 100044, China
[3]Engineering and Research and Development Department, Madrid Metro, 28017 Madrid, Spain
[4]IAC Department, Universidad Politécnica de Madrid (UPM), 28031 Madrid, Spain
[5]COSYS-LEOST, Universite Gustave Eiffel, 77420 Champs-sur-Marne, France

Corresponding author: Ke Guan (kguan@bjtu.edu.cn)

This work was supported in part by the Fundamental Research Funds for the Central Universities under Grant 2020JBZD005, in part by the NSFC under Grant 61771036, Grant U1834210, Grant 61901029, and Grant 61725101; in part by the State Key Laboratory of Rail Traffic Control and Safety Project under Grant RCS2020ZZ005, and in part by the Project Manager EMULRADIO4RAIL under Grant 826152.

ABSTRACT Radio access technologies (RATs) are a key topic in railways, enabling them a better service rendering in terms of shorter headways between trains, higher safety levels and higher customer satisfaction. Very often, these railway RATs need a lot of time to be developed, tested and put into service, which implies a lack of efficiency and bottlenecks in the evolution of railway systems. To solve this situation, an emulation platform that considers both the physical layer and the network (this is, able to emulate the end-to-end chain) is envisaged in the EmulRadio4Rail project. Therefore, the physical layer of many railway scenarios must be emulated, which is a remarkable challenge because railways are very diverse. We see Tapped-Delay Lines (TDL) models as the most efficient way for emulation with the available hardware. In the literature, there are many TDL-based channel models for all the scenarios we considered but one: tunnels. Therefore, in order to fill this gap, we develop a novel TDL model for railway tunnels, considering the impact of the rolling stock (both high-speed railway (HSR) and subway trains). The proposed model allows the full characterization of this scenario in terms of power-delay-profile (PDP), Doppler spectrum and fading characteristics.

INDEX TERMS Channel modeling, propagation, railway communications, tapped-delay-line models, tunnel.

I. INTRODUCTION

In railways, communication systems are becoming more and more necessary now than ever due to the increasing demand for more punctual train services, shorter headways between trains, faster connections to the Internet for passengers and massive sensor networks onboard the trains, among many others [1], [2]. However, recent history has proven that the development of these technologies is very slow (*i.e.* Global System for Mobile Communications – Railway (GSM-R), the dominant radio access technology in railways is almost 20 years old [1]) because the difficulties to do tests on real environments and, on a lesser extent, the absence of economies of scale on a niche market like this. The first problem is targeted by the development of a radio channel emulator which is the main purpose of the EmulRadio4Rail project [3], within the European Shift2Rail initiative.

This radio channel emulator should allow physical connections from the radio access technologies (RATs) being tested on both sides [4]–[7], in order to emulate the whole end-to-end communication system (both the physical and the network layer). The Emulradio4rail platform supports multiple emulation technologies such as Long Term Evolution (LTE) [8], Wireless Fidelity (Wi-Fi), the fifth-generation

The associate editor coordinating the review of this manuscript and approving it for publication was Parul Garg.

mobile communication system (5G) and SatComs [3]. Therefore, with this new tool, the validation process of both existing and new RATs will speed up and some of the current shortcomings of transmission-based signaling technologies like Communication Based Train Control System (CBTC) and European Train Control System (ETCS) will be finally overcome. This will be done in accordance of the Future Railway Mobile Communications System (FRMCS), an initiative that will enable a theoretically easy migration from GSM-R, increase throughput, provide both security and safety functionalities and improved resilience to interferences [9].

In order to validate the FRMCS technologies, an exhaustive process is needed for many different railway applications, like high-speed railway (HSR), subways, tramways, mainline, *etc.*, as well as particular scenarios such as cuttings, tunnels, urban areas, hilly, viaducts and a large etcetera. Railways are very diverse all over the world and a technology aimed to work for the whole sector must address this complexity. Therefore, the RAT emulator must consider many different scenarios to provide support for RATs. The way to do this is to identify reliable and accurate physical-layer channel models for all of them [10]. Due to the available hardware in the Emulradio4rail project and also for efficiency-related considerations that will be discussed in Section II, the models that were decided to be emulated in the project were the tapped-delay line (TDL) based models [11]. As Train-to-Ground (T2G) is the main application of this project, an exhaustive research of published TDL-based models was carried out. Several were found in many different scenarios (as we will see in detail later) but not for tunnels. There are many measurement campaigns and channel models for tunnels [12]–[17] but no one of them is TDL-based. The reason for this is that in this environment there are many multipath components (MPC) very close together and, in order to provide an accurate and useful TDL-based channel model, the needed resolution in the time-domain is very demanding (around 1 ns), which implies 1 GHz bandwidth for the channel sounder [18], [19]. These models are relevant contributions to the research in this field but they are not useful for our channel emulator and, therefore, not useful to validate our new TDL channel model, at least not completely. For example, one of the previous papers [20] develops a model based on measurements in the field but also some validation from ray-tracing measurements. The other railway-related environments (rural, hilly, cutting and viaduct) are outdoor and the associated MPCs are spaced microseconds instead of nanoseconds typical of indoor environments like tunnels. Consequently, in order to fulfill all the requirements for the emulation platform, we decided to retrieve a channel model from ray-tracing (RT) simulations for two different environments: HSR and subway tunnels.

For all of this, the main contributions of this article are twofold:

- Present a TDL-based channel model for railway tunnels, considering as well the influence of the rolling stock in two different setups: large, wide tunnels mainly used for HSR trains and, on the other side, shorter and narrow tunnels for subway trains.
- Identify the influence of the differences between HSR and subway scenarios: size of the tunnel, speed of the train, cross section of the train, etc.

The layout of this paper is as follows: in Section II a brief explanation of the emulation process is provided and a description of the TDL setup is provided as well; in Section III we present the RT simulator and simulation configuration; Section IV reports the methodology of parameter derivation for the TDL models; in Section V we present the obtained models for both types of tunnels and some related discussion on them. Finally, conclusions come in Section VI.

II. EMULATION OF RADIO ACCESS TECHNOLOGIES IN RAILWAYS

A. RAILWAY SCENARIOS

The emulation of RATs in railways is troublesome because there is not a single scenario which could be representative of the whole railway world, so we need to consider many different ones. In this research work, we have significantly simplified this diversity and we have considered five different scenarios [21]–[23]:

- Rural: this is the most common one in both mainline and HSR lines [24].
- Viaduct: due to the inability of HSR trains to run on very high ramps, on these lines it is very common to construct viaducts [25], [26].
- Cutting: very useful to decrease the impact on neighboring areas and to ease transitions from and to tunnels [27].
- Hilly terrain: very common in several railway lines around the world [28], [29].
- Tunnel: this is the most likely one in metropolitan railways (subways) but also common in HSR lines [16], [30]. In this scenario we will focus from now on.

Therefore, there is a high chance that every railway line in the world could be characterized as an ensemble of several stretches of the five scenarios considered above. For more details on each one of them, please see Deliverable 1.3 of the EmulRadio4Rail Project [3].

B. MODELS

After the definition of the scenarios to be considered in the emulation process, we need to explain how this emulation will be performed. The aim of the platform is the end-to-end emulation of the RAT, so both a channel emulator and a network emulator are needed. From now on, we will focus on physical layer aspects only (i.e. channel emulator). Details on this platform can be found in our previous papers [12], [31].

Perhaps the most efficient way to emulate a wideband channel is using TDL models [11]. The idea behind this is the following: MPCs arrive at the receiver (Rx) in many different (and discrete) moments in time and each one of them has its own power figure as depicted in Fig. 1. It is assumed that within each tap the spectrum is flat (*i.e.* there is no frequency selectivity) and that all taps are not correlated with each other.

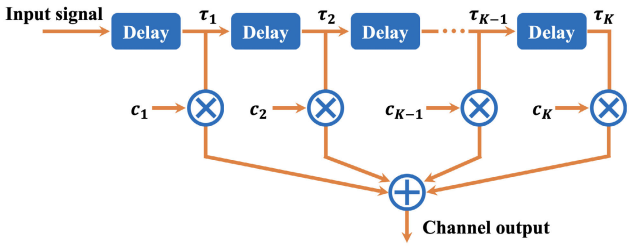

FIGURE 1. Schematic of the tapped-delay-line channel model.

Therefore, we can model the channel impulse response (CIR) as the sum of delayed MPCs:

$$h(\tau, t) = \sum_{k=1}^{K} c_k \delta(\tau - \tau_k) \tag{1}$$

where τ is the delay, t is time, c_k is the complex coefficient associated to each one of the K taps. For practical reasons, taps with a power below a threshold are discarded and all MPCs within a time frame are grouped together into a single tap. All these practicalities, including both the tap width and power threshold, are explained in detail in Section IV.

Moreover, for each one of the taps we must consider the Doppler spectrum which is the distribution of the frequency shifts associated to each MPC that arrives at the Rx. This is of great importance in vehicular scenarios like railways (in particular, HSR trains can run up to 350 km/h, probably faster in the mid-term). For more details on TDL models any classical text on channel modelling and measurement like for example [11] is a good reference.

Once we had a clear decision on the type of wideband model to be used, we performed an exhaustive literature survey of existing TDL-based models for railway scenarios. The outcome of this survey is that there are many published TDL models for all railway scenarios but not even one for tunnels. We only considered those who included complete information about the Doppler spectrum, speed range, bandwidth, diversity scheme, as well as the more obvious number of taps, delay, frequency range and relative power associated to the taps. Based on this information, we chose the most suitable ones for our emulation platform. All the details of the models and also the assessment on the suitability of each one of them has been already published as a deliverable report in our project [32].

III. RAY-TRACING AND SIMULATION PROCEDURE

A high-performance computing (HPC) cloud-based ray-tracing simulator (CloudRT) is utilized in this study. The simulator is developed by the State Key Laboratory of Rail Traffic Control and Safety, Beijing Jiaotong University [33]. It is based on the RT technique, which considers the antenna patterns, the existence of the scatterers, locations of transmitter (Tx) and Rx, and various propagation mechanisms. The complete RT simulation process is that the user first needs to reconstruct the three-dimensional (3D) model of the target scenario and the scatterers and define the electromagnetic (EM) parameters of the material, then set the simulation frequency, propagation mechanism, transceiver and scatterers motion trajectory, antenna type and other parameters, and finally start the RT simulation. After calibrating the geometry of the 3D environment model, and determining the EM parameters of objects/materials and the dominant propagation mechanisms, intensive RT simulations can be conducted with various Tx/Rx deployments as well as various combinations of the objects, which breaks the limits of the measurement [34], [35]. Based on the simulation results, the ray information can be captured, and moreover the TDL model parameters can be extracted. CloudRT has been validated by extensive measurements in various railway environments [23], [36]. In our recent work [37], [38], CloudRT has been validated at 30 GHz and 90 GHz in HSR outdoor and tunnel environments, respectively. More details of CloudRT can be found in http://www.raytracer.cloud.

A. SCENARIO AND SCATTERERS MODELING

In this study, the simplified HSR and subway tunnel scenarios are reconstructed. The cross-sections of the two tunnels in the simulations are shown in Fig. 2. W_1 and H are the width and height of the tunnel, W_2 is the spacing of rail and W_3 is the width of the rail. As the dual-lines are considered, R is the distance between the rail and the wall. The length of each tunnel in the simulation is 3000 m. As shown in Fig. 3, two types of train bodies are modeled. The width, height, and length of the HSR train are 2.942 m, 3.70 m and 200 m, respectively. The width, height, and length of the subway train are 2.8 m, 3.25 m and 55.049 m, respectively.

B. RT SIMULATION CONFIGURATION

In this study, Tx is deployed closed to the wall of the tunnel, and Rx is placed on the top of the train body. As for rectangle HSR tunnel, Tx and Rx are placed at a height of 4.55 m and 4.05 m, respectively. As for rectangular subway tunnel, Tx and Rx are placed at a height of 4.10 m and 3.60 m, respectively. Two antennas are employed at both the Tx and Rx, and the two antenna elements are spaced apart with an inter-distance of $\lambda/2$. Considering the tradeoff between computing resource and accuracy, up to 6-order reflection is deployed in this simulation. The specific deployment of the tunnel is shown in Fig. 4. TABLE 1 summarizes the simulation configuration. In Multiple-Input Multiple-Output (MIMO) channel, 4 subchannels are set (as shown in Fig. 5), which constitute the Channel Matrix (2).

$$H = \begin{bmatrix} h_{11} & h_{12} \\ h_{21} & h_{22} \end{bmatrix} \tag{2}$$

The considered materials include the concrete (the tunnel) and metal (the train body and rails). The EM parameters of the mentioned materials are provided by the State Key Laboratory of Rail Traffic Control and Safety, Beijing Jiaotong University, as listed in TABLE 2.

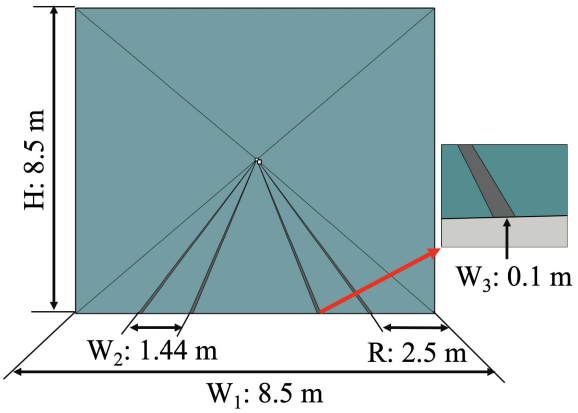

(a) Rectangle HSR tunnel

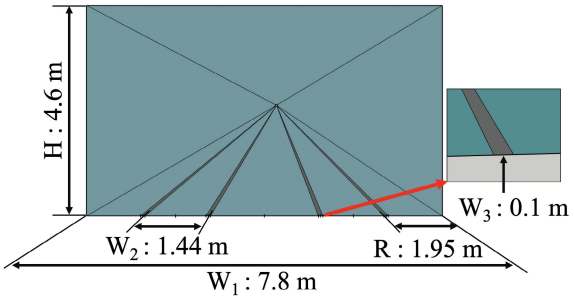

(b) Rectangle subway tunnel

FIGURE 2. Cross-sections of the tunnels.

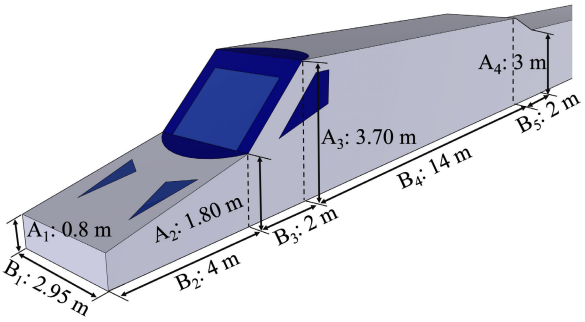

(a) HSR train

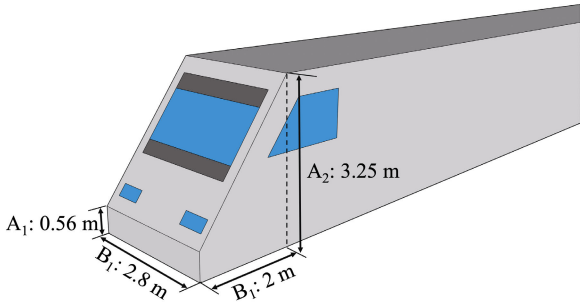

(b) Subway train

FIGURE 3. 3D models of the train bodies in the simulation.

IV. TDL MODEL PARAMETERS DERIVATION

A. DELAY VALUE AND AVERAGE GAIN OF TAPS

In RT simulations, a pair of Tx/Rx is simulated as a single snapshot with the predefined configurations. A simulation task for an environment model is composed of N_s snapshots. For each snapshot, the intrinsic results include the number of rays N_r, ray energy $E(s, j)$ and the delay of each ray $\tau(s, j)$ (s is the index of snapshot, and j is the index of ray in snapshot s) [39]. In order to achieve a time-domain resolution

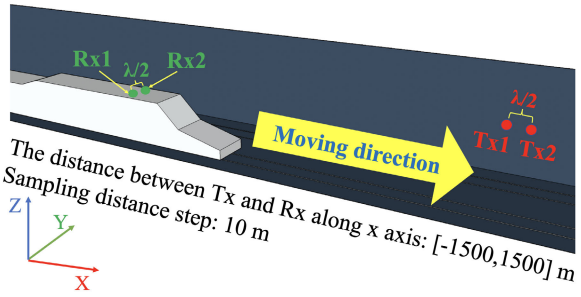

(a) Rectangle HSR tunnel

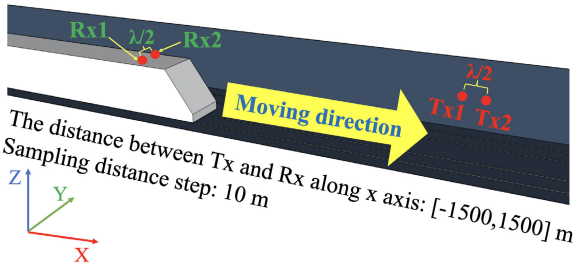

(b) Rectangle subway tunnel

FIGURE 4. The deployment of Tx and Rx antennas in the simulation.

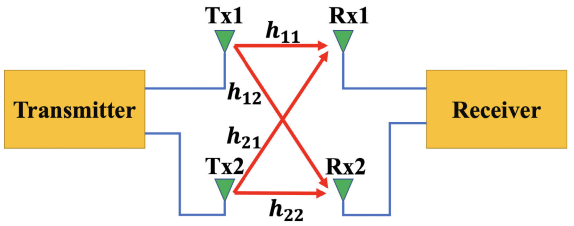

FIGURE 5. MIMO system.

TABLE 1. Simulation configuration.

Parameter	Value
Center frequency	2.4 GHz
Sampling distance step	10 m
Tx-Rx distance along the x-axis	[-1500,1500] m
Tx / Rx antenna height in HSR tunnel	4.55 m, 4.05 m
Tx / Rx antenna height in subway tunnel	4.10 m, 3.60 m
Antenna type	Vertical polarized omni-directional, 0 dBi gain
Element spacing	$\lambda/2$
Propagation mechanism	Direct path, reflection up to the 6^{th} order

TABLE 2. The electromagnetic parameters of main objects.

Object Name	Material	ε_r	$tan\delta$
Tunnel	Concrete	7.9	0.082
Rail	Metal	1	10^7
Train body	Metal	1	10^7

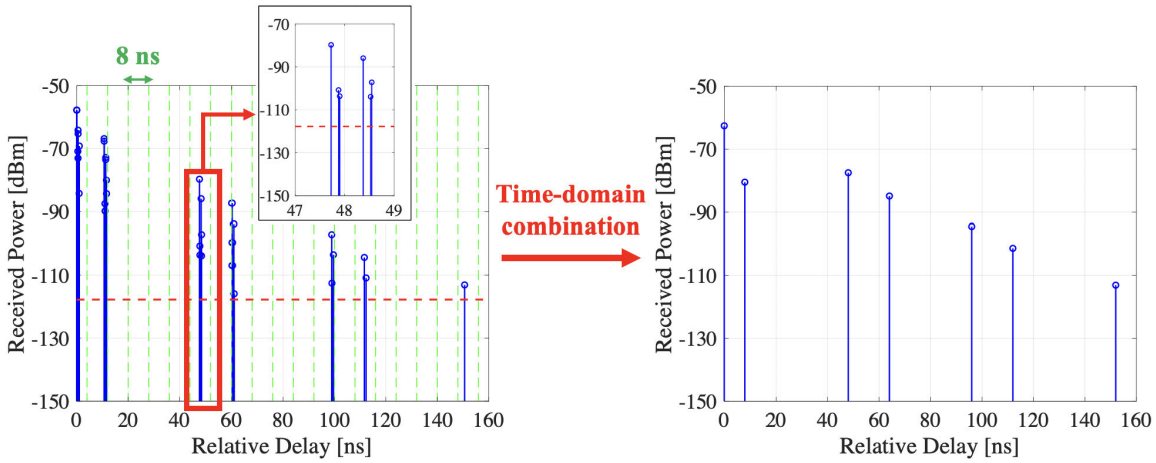

FIGURE 6. An example of combining the multipaths to obtain the CIR in subway tunnel scenario. The 8 ns resolution is given as the green dotted line and the threshold of −60 dB is given as the red dotted line.

as high as 1 ns for a channel model, there are two types of simulations: the frequency-domain RT simulation with a bandwidth of 1 GHz, or the time-domain RT simulation. Considering that it is not feasible to use 1 GHz bandwidth at such a low frequency band–2.4 GHz in reality for communications, so in order to achieve a sufficiently high multipaths resolution, we use the time-domain RT simulation, because its time resolution is only limited by the number of CPU bits of the computer, and its resolvable time duration is much shorter than the delay difference between two adjacent multipaths in the simulation. As shown in Fig. 6, as an example, numerical multipaths between 48 and 49 ns are with much shorter delay differences than 1 ns but still can be resolvable by the time-domain RT simulation. Since the time-domain resolution of the emulator that is aiming to use our channel model is 8 ns, we combine the multipaths (with the threshold of 60 dB below the strongest ray power) within every $\Delta\tau$ of 8 ns duration in time-domain to obtain the CIR for further modeling (as shown in Fig. 6), which can be expressed as

$$h(s, m\Delta\tau) = \sum_{J} E(s, j), \quad J = \{j | m\Delta\tau - \frac{\Delta\tau}{2} \leq \tau(s, j) < m\Delta\tau + \frac{\Delta\tau}{2}, m \geq 0\} \tag{3}$$

where m is the delay bin index. From which, we define the instantaneous power delay profile (PDP) as

$$P(s, m\Delta\tau) = |h(s, m\Delta\tau)|^2 \tag{4}$$

where $|\cdot|$ denotes the absolute value. The instantaneous gain for the Tx-Rx link is expressed as

$$P_G(s) = \sum_{m=1}^{M_s} P(s, m\Delta\tau) \tag{5}$$

where M_s is the number of delay bins in snapshot s. After removing the mean value of $P_G(s)$ from $h(s, m\Delta\tau)$ within the bin,the normalized CIR $h_{norm}(s, m\Delta\tau)$ can be obtained as

$$h_{norm}(s, m\Delta\tau) = \frac{h(s, m\Delta\tau)}{\sqrt{\frac{1}{N_s}\sum_{s=1}^{N_s} P_G(s)}} \tag{6}$$

This operation is done to reduce the distance dependence and shadowing effects. The instantaneous normalized PDP is expressed as

$$P_{norm}(s, m\Delta\tau) = |h_{norm}(s, m\Delta\tau)|^2 \tag{7}$$

The averaged normalized PDP is then calculated as

$$P_{ave}(m\Delta\tau) = \frac{1}{N_s}\sum_{s=1}^{N_s} P_{norm}(s, m\Delta\tau) \tag{8}$$

The instantaneous and averaged normalized PDPs of h_{22} for subway tunnel scenario are presented in Fig. 7. For determining the number of taps in the model, the threshold

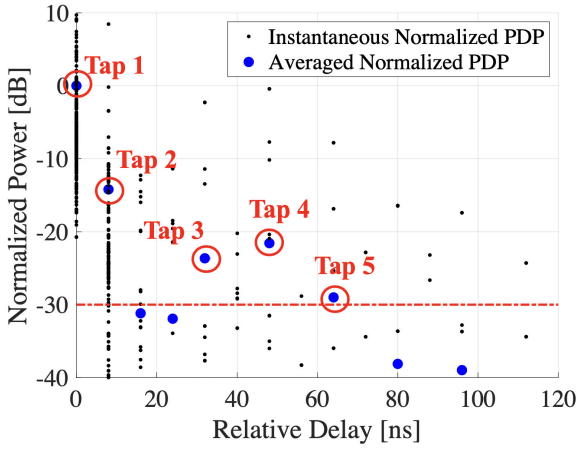

FIGURE 7. An example of instantaneous and averaged normalized PDPs in subway tunnel scenario. The threshold of −30 dB is given as the red dotted line.

of 30 dB below the strongest tap power is used. Then the averaged normalized power gains and the delay values can be obtained through the delay bin index of the remaining taps. For example, as shown in Fig. 7, the number of taps is 5. The delay bin indexes are $l = m = 1, 2, 5, 6, 7$, delay values are calculated from $l\Delta\tau$, and averaged power gains, $P_l = P_{ave}(l\Delta\tau)$, are from Equation (8).

The normalized amplitude is given by $|\alpha(s, l\Delta\tau)|$, which can be calculated as

$$\alpha(s, l\Delta\tau) = \frac{h_{norm}(s, l\Delta\tau)}{\sqrt{P_l}} \tag{9}$$

$$P_l = \frac{1}{N_s}\sum_{s=1}^{N_s} |h_{norm}(s, l\Delta\tau)|^2 \tag{10}$$

where l is the index of remaining taps.

B. DOPPLER SPECTRUM OF TAPS

Different normalization methods are used when calculating the Doppler spectrum. For all snapshots, the scalar sum of power of rays $P(s)$ for snapshot s is used to normalize the power of effective rays $P_{norm-ray}(s, j)$, so that the distance-dependent path loss is removed, which can be expressed as

$$P(s) = \sum_{j=1}^{N_r} |E(s, j)|^2 \tag{11}$$

$$P_{norm-ray}(s, j) = \frac{|E(s, j)|^2}{P(s)} \tag{12}$$

The corresponding Doppler shift of each ray in snapshot s ($f_d(s, j)$) can be expressed as

$$f_d(s, j) = -f_c \cdot \frac{\vec{v}_{Rx}(s) \cdot \vec{k}(s, j)}{c} \tag{13}$$

where f_c is the center frequency, $\vec{v}_{Rx}(s)$ is the velocities of Rx, $\vec{k}(s, j)$ is the unit vector along the direction of the ray departing from the Tx, scattering point or reflecting point towards the Rx, and c is the speed of light. Then, all the normalized effective rays and corresponding Doppler shift of each ray in each snapshot are grouped by the time delay interval 8 ns to form several taps of rays.

For each tap, we make statistical analysis for the power and Doppler shift of all the rays within this tap of all the snapshots. Jakes model [40] is used to fit the Doppler spectrum within each tap of all the snapshots, which can be modeled as:

$$S(f_d(s, j)) = \frac{2\sigma^2(s, l)}{\pi f_{max}\sqrt{1 - \frac{f_d(s,j)}{f_{max}}}}, \quad \{j | l\Delta\tau - \frac{1}{2}\Delta\tau \leq \tau(s, j) < \Delta\tau + \frac{1}{2}, l \geq 0\} \tag{14}$$

where $2\sigma^2(s, l)$ is the scattering component power of tap l in snapshot s, f_{max} is the maximum Doppler shift of the HSR or subway train.

V. CHANNEL MODELS

In this section, we provide the obtained channel models, in terms of the parameters defined above for both types of tunnels (HSR and subway).

A. HIGH-SPEED RAILWAY TUNNELS

In Tables 3, 4, 5, and 6, the MIMO 2 × 2 TDL model for the HSR tunnel is considered. In these tables, we can see both the power and delay associated to each of the 11 taps which comprise each of the subchannels of the 2×2 MIMO channel. The PDP for h_{11} is shown in Fig. 8. We can see that, as it was expected, the maximum power is related to $\tau = 0$ ns (the graph is not normalized to 0 dB but in absolute received power in dBm) which is the LOS component. Given that the Tx is in the middle of the tunnel, the maximum received power is obtained at the central snapshot of the simulations. Due to the limitation introduced in the time resolution (to 8 ns, as we discussed in Section IV), the number of MPCs that we are able to solve is limited. In this case, we obtain 11 taps but for subway tunnels, we only get 5 with a significant power figure (the power threshold is set at 30 dB below the maximum tap).

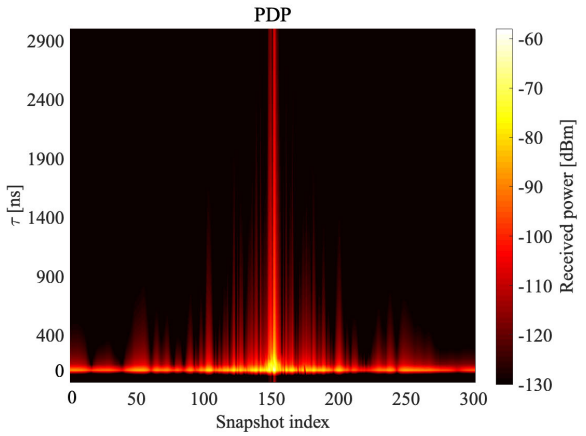

FIGURE 8. PDP for h_{11} in HSR tunnel.

The fading distribution, which fits better to the results is not Rayleigh as it could be foreseen, but Weibull and the values of the distribution parameters for each tap are provided as well in Tables 3–6. Regarding the better fitting to a Weibull distribution rather than to a Rayleigh, the reason is that scatterers are not uniformly distributed in the tunnel because they come from the tunnel walls, which was studied in the literature [41] as well as in some experiments in the field [42] and it is the main assumption related to Weibull Distribution (15).

$$pdf(|\alpha|; \beta_w, \Omega_{weib}) = \frac{\beta_w}{\Omega_{weib}}|\alpha|^{\beta_w - 1} \cdot e^{(-\frac{|\alpha|^{\beta_w}}{\Omega_{weib}})} \tag{15}$$

The other parameter of this distribution β_w describes the average fading power. As it is known from the first descriptions of the Weibull distribution, Rayleigh distribution is a particular case ($\beta_w = 2$) of it. β_w accounts the fading severity, increasing the fading as β_w decreases.

TABLE 3. TDL parameters of h_{11} for HSR tunnel scenario.

Tap No.	Delay (ns)	Path Power		Fading Distribution		Doppler Spectrum			
		(lin.)	(dB)	Weibull		Shape	Fitting Model of σ_{Jakes}	μ_{LL}	σ_{LL}
				β_ω	Ω_{weib}				
1	0	1	0	0.17	0.69	Jakes	Log-Logistic	0.0232	0.2397
2	8	0.2550	-5.9354	0.69	0.38	Jakes	Log-Logistic	-1.1955	0.2263
3	16	0.1645	-7.8387	0.52	0.35	Jakes	Log-Logistic	-1.1289	0.1863
4	24	0.1242	-9.0596	0.36	0.44	Jakes	Log-Logistic	-0.9383	0.2453
5	32	0.0472	-13.2576	0.48	0.78	Jakes	Log-Logistic	-0.7976	0.3371
6	40	0.0313	-15.0394	0.59	1	Jakes	Log-Logistic	-0.6182	0.2581
7	48	0.0129	-18.8940	0.48	0.94	Jakes	Log-Logistic	-0.6448	0.1544
8	56	0.0266	-16.8539	0.56	1.04	Jakes	Log-Logistic	-0.5082	0.1022
9	64	0.0140	-18.5330	0.62	1.36	Jakes	None	σ_{Jakes}	
								0.4654	
10	72	0.0033	-24.8490	0.92	2.78	Jakes	None	0.4081	
11	80	0.0017	-27.7257	0.88	3.35	Jakes	None	0.4435	

TABLE 4. TDL parameters of h_{12} for HSR tunnel scenario.

Tap No.	Delay (ns)	Path Power		Fading Distribution		Doppler Spectrum			
		(lin.)	(dB)	Weibull		Shape	Fitting Model of σ_{Jakes}	μ_{LL}	σ_{LL}
				β_ω	Ω_{weib}				
1	0	1	0	1.17	0.69	Jakes	Log-Logistic	0.0232	0.2397
2	8	0.2563	-5.9125	0.69	0.38	Jakes	Log-Logistic	-1.1955	0.2269
3	16	0.1654	-7.8156	0.52	0.35	Jakes	Log-Logistic	-1.2885	0.1851
4	24	0.1240	-9.0657	0.36	0.44	Jakes	Log-Logistic	-0.9382	0.2452
5	32	0.0464	-13.3303	0.48	0.78	Jakes	Log-Logistic	-0.7983	0.3357
6	40	0.0314	-15.0252	0.59	1.01	Jakes	Log-Logistic	-0.6083	0.2638
7	48	0.0123	-19.0947	0.50	0.94	Jakes	Log-Logistic	-0.6447	0.1537
8	56	0.0207	-16.8403	0.56	1.03	Jakes	Log-Logistic	-0.5084	0.1045
9	64	0.0134	-18.7221	0.60	1.27	Jakes	None	σ_{Jakes}	
								0.4538	
10	72	0.0039	-24.1345	0.90	2.76	Jakes	None	0.4194	
11	80	0.0017	-27.8016	0.86	3.17	Jakes	None	0.4434	

TABLE 5. TDL Parameters of h_{21} for HSR tunnel scenario.

Tap No.	Delay (ns)	Path Power		Fading Distribution		Doppler Spectrum			
		(lin.)	(dB)	Weibull		Shape	Fitting Model of σ_{Jakes}	μ_{LL}	σ_{LL}
				β_ω	Ω_{weib}				
1	0	1	0	1.15	0.68	Jakes	Log-Logistic	0.0333	0.2369
2	8	0.2556	-5.9253	0.70	0.37	Jakes	Log-Logistic	-1.1919	0.2252
3	16	0.1440	-8.4177	0.53	0.36	Jakes	Log-Logistic	-1.2911	0.1878
4	24	0.1229	-9.1056	0.36	0.43	Jakes	Log-Logistic	-0.9459	0.2436
5	32	0.0497	-13.0347	0.49	0.81	Jakes	Log-Logistic	-0.7684	0.3655
6	40	0.0363	-14.3972	0.57	1.02	Jakes	Log-Logistic	-0.6153	0.2563
7	48	0.0132	-18.8071	0.49	0.89	Jakes	Log-Logistic	-0.6381	0.1596
8	56	0.0070	-21.5761	0.65	1.38	Jakes	Log-Logistic	-0.5238	0.1158
9	64	0.0149	-18.2809	0.59	1.35	Jakes	None	σ_{Jakes}	
								0.4530	
10	72	0.0039	-24.0510	0.89	2.70	Jakes	None	0.4189	
11	80	0.0017	-27.7583	0.85	2.91	Jakes	None	0.4419	

Consequently, looking at the measured β_w parameter in Tables 3–6, we can see that the fading severity in this scenario is always much worse than Rayleigh, which gives an idea of how extreme and challenging the tunnel scenario is. Regarding the power distribution of the fading, we see that the relative power from the 3^{rd}-4^{th} tap increases monotonically. This can be explained in the reduction of MPCs and also on its heterogeneity (in terms of followed paths, reflections, etc.) that arrive at the Rx as the tap-index increases, which means that the variance of the power of the MPCs is presumably higher.

The maximal speed for the train is 350 km/h, and the carrier frequency is 2.4 GHz which leads to a maximal Doppler shift of $\pm$800 Hz. Regarding the Doppler spectrum, all the taps in the models are Jakes' shaped and the distribution which fits better the Jakes' σ related to the model is log-logistic

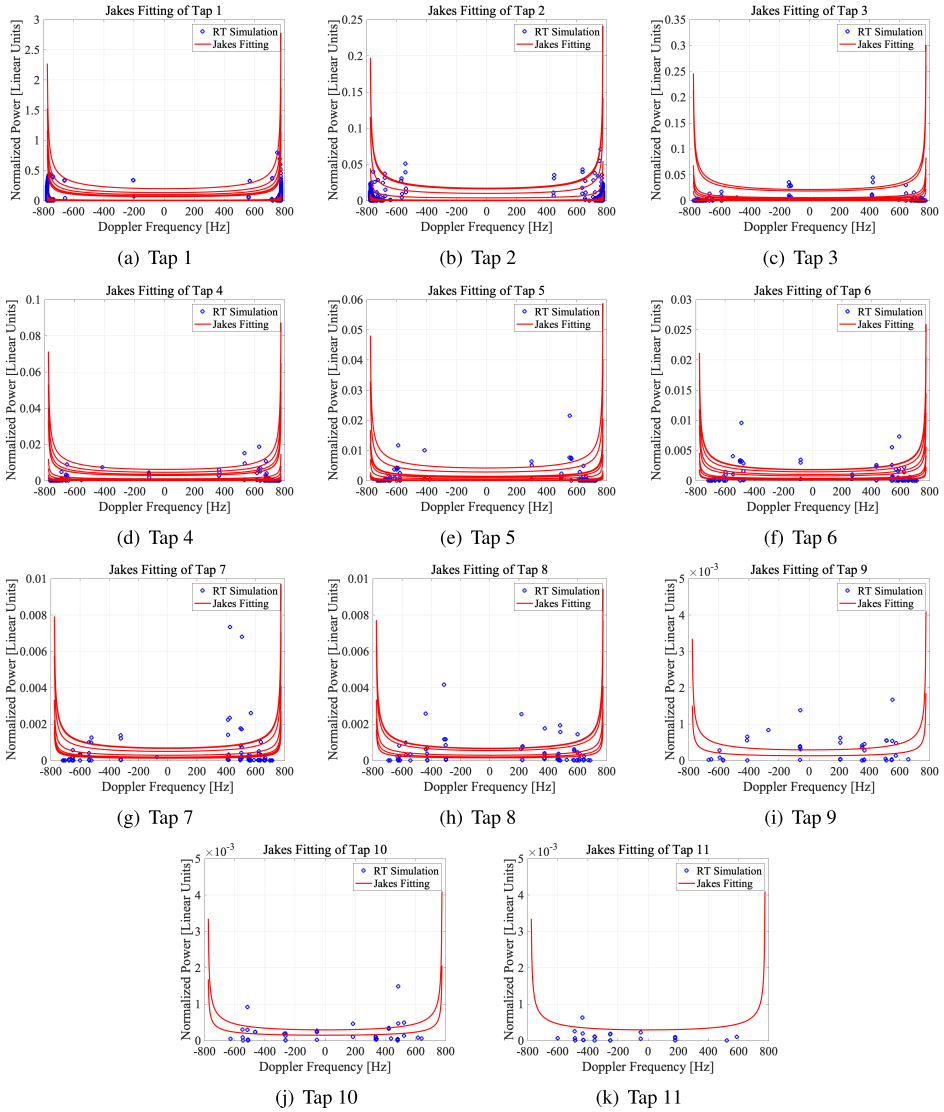

(a) Tap 1 (b) Tap 2 (c) Tap 3

(d) Tap 4 (e) Tap 5 (f) Tap 6

(g) Tap 7 (h) Tap 8 (i) Tap 9

(j) Tap 10 (k) Tap 11

FIGURE 9. The Doppler shift and its Jakes fitting model of the h_{11} channel for HSR scenario.

(see tables 3–6 for more details and values of related parameters), and its probability density function (PDF) is:

$$pdf(\sigma(s,l);\mu_{LL},\sigma_{LL}) = \frac{1}{\sigma_{LL}} \cdot \frac{1}{\sigma(s,l)} \cdot \frac{e^z}{(1+e^z)^2} \quad (16)$$

$$z = \frac{log(\sigma(s,l)) - \mu_{LL}}{\sigma_{LL}} \quad (17)$$

where μ_{LL} is the mean of logarithmic value, σ_{LL} is the scale parameter of logarithmic value, and $\sigma(s,l)$ is the fitting parameters of Jakes model for every taps. If the number of $\sigma(s,l)$ of tap l is less than 15, one Jakes model is adopted to fit the Doppler shift of all the rays within this tap l. The obtained shifts for each tap of the TDL model and the statistical fit are both shown in Fig. 9.

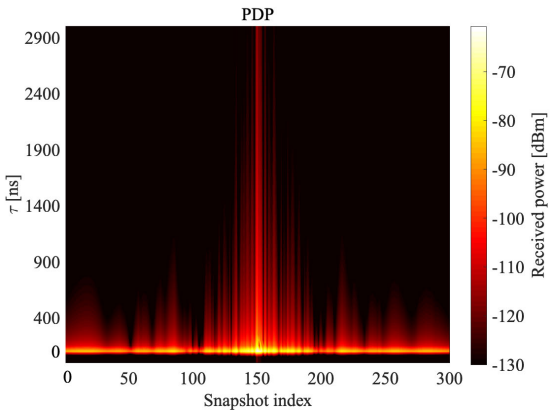

FIGURE 10. PDP for h_{11} in subway tunnel.

B. SUBWAY TUNNELS

The procedure for these simulations is the same as for HSR trains but this time we have a shorter tunnel, slower trains (110 km/h) and smaller trains as well (See Table 7–10 for all the simulation details). As in the HSR scenario we have a dominant line-of-sight (LOS) path in terms of power but

TABLE 6. TDL parameters of h_{22} for HSR tunnel scenario.

Tap No.	Delay (ns)	Path Power		Fading Distribution		Doppler Spectrum			
		(lin.)	(dB)	Weibull		Shape	Fitting Model of σ_{Jakes}	μ_{LL}	σ_{LL}
				β_ω	Ω_{weib}				
1	0	1	0	1.15	0.68	Jakes	Log-Logistic	0.0333	0.2368
2	8	0.2551	-5.9331	0.70	0.37	Jakes	Log-Logistic	-1.1915	0.2258
3	16	0.1472	-8.3209	0.53	0.35	Jakes	Log-Logistic	-1.2905	0.1863
4	24	0.1227	-9.1117	0.36	0.43	Jakes	Log-Logistic	-0.9459	0.2435
5	32	0.0498	-13.0290	0.49	0.81	Jakes	Log-Logistic	-0.7689	0.3655
6	40	0.0365	-14.3812	0.57	1.03	Jakes	Log-Logistic	-0.6076	0.2609
7	48	0.0129	-18.8986	0.49	0.86	Jakes	Log-Logistic	-0.6396	0.1604
8	56	0.0071	-21.4619	0.65	1.37	Jakes	Log-Logistic	-0.5239	0.1157
9	64	0.0149	-18.2646	0.59	1.35	Jakes	None	σ_{Jakes} 0.4533	
10	72	0.0039	-24.0733	0.89	2.70	Jakes	None	0.4189	
11	80	0.0016	-27.8333	0.84	2.79	Jakes	None	0.4417	

TABLE 7. TDL Parameters of h_{11} for subway tunnel scenario.

Tap No.	Delay (ns)	Path Power		Fading Distribution		Doppler Spectrum				
		(lin.)	(dB)	Weibull		Shape	Fitting Model of σ_{Jakes}	α	c	k
				β_ω	Ω_{weib}					
1	0	1	0	1.22	0.69	Jakes	Burr	0.6119	28.6175	0.2131
2	8	0.0377	-14.2312	0.68	0.44	Jakes	Burr	0.1568	39.1621	0.1061
3	32	0.0043	-23.6337	0.50	1.11	Jakes	None	σ_{Jakes} 0.1329		
4	48	0.0070	-21.5570	0.57	1.25	Jakes	None	0.2275		
5	64	0.0013	-28.9994	0.96	4.02	Jakes	None	0.1991		

TABLE 8. TDL parameters of h_{12} for subway tunnel scenario.

Tap No.	Delay (ns)	Path Power		Fading Distribution		Doppler Spectrum				
		(lin.)	(dB)	Weibull		Shape	Fitting Model of σ_{Jakes}	α	c	k
				β_ω	Ω_{weib}					
1	0	1	0	1.22	0.69	Jakes	Burr	0.6121	28.5526	0.2134
2	8	0.0378	-14.2202	0.68	0.44	Jakes	Burr	0.1568	40.4683	0.1025
3	32	0.0043	-23.6271	0.50	1.11	Jakes	None	σ_{Jakes} 0.1325		
4	48	0.0070	-21.5352	0.57	1.25	Jakes	None	0.2275		
5	64	0.0013	-28.9919	0.96	4.02	Jakes	None	0.1991		

TABLE 9. TDL parameters of h_{21} for subway tunnel scenario.

Tap No.	Delay (ns)	Path Power		Fading Distribution		Doppler Spectrum				
		(lin.)	(dB)	Weibull		Shape	Fitting Model of σ_{Jakes}	α	c	k
				β_ω	Ω_{weib}					
1	0	1	0	1.19	0.69	Jakes	Burr	0.6179	19.7439	0.3316
2	8	0.0373	-14.2777	0.67	0.47	Jakes	Burr	0.1575	40.0865	0.1032
3	32	0.0045	-23.5007	0.53	1.17	Jakes	None	σ_{Jakes} 0.1436		
4	48	0.0075	-21.2624	0.57	1.26	Jakes	None	0.2165		
5	64	0.0013	-28.7612	0.96	4.02	Jakes	None	0.1991		

here we have less resolvable MPCs (5 instead of 11 as we had in HSR). This is due to the size of the tunnel which tends to concentrate more power on the LOS component. This is depicted in Fig. 10 where it is even hard to appreciate the power for the other MPCs rather than the direct one.

The fading distribution is Weibull as in the HSR scenario, which makes sense because both tunnels share a common propagation environment, with scatterers not uniformly distributed around the Rx. β_w figures are very similar in both cases, a little higher in subway which means less severe

TABLE 10. TDL parameters of h_{22} for subway tunnel scenario.

Tap No.	Delay (ns)	Path Power		Fading Distribution		Doppler Spectrum				
		(lin.)	(dB)	Weibull		Shape	Fitting Model of σ_{Jakes}	α	c	k
				β_ω	Ω_{weib}					
1	0	1	0	1.19	0.69	Jakes	Burr	0.6182	19.6848	0.3323
2	8	0.0318	-14.9759	0.67	0.49	Jakes	Burr	0.1575	40.4733	0.1021
3	32	0.0045	-23.4983	0.53	1.17	Jakes	None	σ_{Jakes} 0.1441		
4	48	0.0075	-21.2391	0.57	1.27	Jakes	None	0.2171		
5	64	0.0013	-28.7540	0.96	4.02	Jakes	None	0.1991		

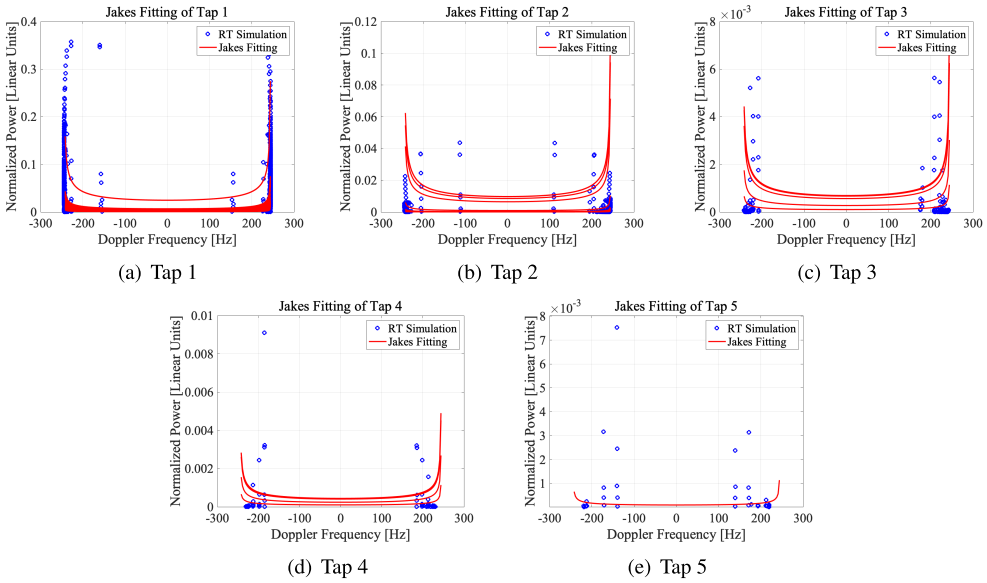

(a) Tap 1 (b) Tap 2 (c) Tap 3

(d) Tap 4 (e) Tap 5

FIGURE 11. The Doppler shift and its Jakes fitting model of the h_{11} channel for subway scenario.

fading. In both cases, the fading is worse than Rayleigh ($\beta_w < 2$). Regarding the Doppler spectrum, obviously, the maximum shift is lower (244 Hz) than in HSR because the train speed is lower (110 km/h). Regarding the distribution fitting, for the first two taps, the best fit is a Burr distribution. For the other three taps, there is no enough resolvable data points to do a proper fit (the number of $\sigma(s, l)$ of tap l is less than 15). Burr distribution is depicted in (18). The Doppler spectrum associated to the five taps of this model is depicted in Fig. 11.

$$pdf(\sigma(s,l);\alpha,c,k) = \frac{\frac{k\cdot c}{\alpha}(\frac{\sigma(s,l)}{\alpha})^{c-1}}{(1+(\frac{\sigma(s,l)}{\alpha})^{c})^{k+1}}, \quad \alpha>0,\quad c>0,\ k>0 \qquad (18)$$

where α is the scale parameter; c and k are both the shape factors. In Tables 7–10, we provide all the parameters related to this 2×2 MIMO TDL model.

VI. CONCLUSION

In this paper we have presented a complete TDL-based channel model for railway tunnels considering two different scenarios: HSR and subway tunnels. The differences among them are subtle but important for real-world technical and engineering problems. The influence of the usual rolling stock that runs through these tunnels has been included in the model as well as other details in order to be more realistic.

The differences in the resolvable paths between HSR and subway tunnels are worth mentioning (11 and 5 for HSR and subway tunnels, respectively) as well as the dominance of the direct path in both cases but on a larger extent in the subway tunnel. The proposed TDL model can be embedded into emulators for an end-to-end emulation of RATs in tunnel environments. This will effectively help the design, development, and validation of FRMCS technologies.

REFERENCES

[1] J. Moreno, J. M. Riera, L. D. Haro, and C. Rodriguez, "A survey on future railway radio communications services: Challenges and opportunities," *IEEE Commun. Mag.*, vol. 53, no. 10, pp. 62–68, Oct. 2015.

[2] Y. Liu, C.-X. Wang, C. Lopez, and X. Ge, "3D non-stationary wideband circular tunnel channel models for high-speed train wireless communication systems," *Sci. China Inf. Sci.*, vol. 60, no. 8, Aug. 2017, Art. no. 082304.

[3] IFSTTAR. *Emulradio4rail Project*. Accessed: Aug. 20, 2020. [Online]. Available: http://www.emulradio4rail.eu

[4] Y. Liu, C.-X. Wang, C. F. Lopez, G. Goussetis, Y. Yang, and G. K. Karagiannidis, "3D non-stationary wideband tunnel channel models for 5G high-speed train wireless communications," *IEEE Trans. Intell. Transp. Syst.*, vol. 21, no. 1, pp. 259–272, Jan. 2020.

[5] Y. Liu, C.-X. Wang, and J. Huang, "Recent developments and future challenges in channel measurements and models for 5G and beyond high-speed train communication systems," *IEEE Commun. Mag.*, vol. 57, no. 9, pp. 50–56, Sep. 2019.
[6] Y. Liu, C.-X. Wang, J. Huang, J. Sun, and W. Zhang, "Novel 3-D non-stationary mmWave massive MIMO channel models for 5G high-speed train wireless communications," *IEEE Trans. Veh. Technol.*, vol. 68, no. 3, pp. 2077–2086, Mar. 2019.
[7] S. Wu, C.-X. Wang, E.-H.-M. Aggoune, M. M. Alwakeel, and X. You, "A general 3-D non-stationary 5G wireless channel model," *IEEE Trans. Commun.*, vol. 66, no. 7, pp. 3065–3078, Jul. 2018.
[8] K. Guan, Z. Zhong, and B. Ai, "Assessment of LTE-R using high speed railway channel model," in *Proc. 3rd Int. Conf. Commun. Mobile Comput.*, Apr. 2011, pp. 461–464.
[9] UIC. *Future Railway Mobile Communication System (FRMCS)*. Accessed: Aug. 20, 2020. [Online]. Available: https://uic.org/rail-system/frmcs/
[10] B. Ai, X. Cheng, T. Kürner, Z.-D. Zhong, K. Guan, R.-S. He, L. Xiong, D. W. Matolak, D. G. Michelson, and C. Briso-Rodriguez, "Challenges toward wireless communications for high-speed railway," *IEEE Trans. Intell. Transp. Syst.*, vol. 15, no. 5, pp. 2143–2158, Oct. 2014.
[11] A. F. Molisch, *Wireless Communication*, 2nd ed. Hoboken, NJ, USA: Wiley, 2011.
[12] J. M. Garcia-Loygorri, S. Kharbech, L. Clavier, R. Kassi, R. Torrego, A. Arriola, I. Val, M. Berbineau, J. Soler, and Y. Yan, "Emulation of end-to-end communications systems in railway scenarios: Physical layer results," in *Proc. 14th Eur. Conf. Antennas Propag. (EuCAP)*, Mar. 2020, pp. 1–5.
[13] L. Zhang, C. Briso, J. R. O. Fernandez, J. I. Alonso, C. Rodriguez, J. M. Garcia-Loygorri, and K. Guan, "Delay spread and electromagnetic reverberation in subway tunnels and stations," *IEEE Antennas Wireless Propag. Lett.*, vol. 15, pp. 585–588, 2016.
[14] X. Cai, X. Yin, X. Cheng, and A. Perez Yuste, "An empirical random-cluster model for subway channels based on passive measurements in UMTS," *IEEE Trans. Commun.*, vol. 64, no. 8, pp. 3563–3575, Aug. 2016.
[15] J. Yu, W. Chen, F. Li, C. Li, K. Yang, Y. Liu, and F. Chang, "Channel measurement and modeling of the small-scale fading characteristics for urban inland river environment," *IEEE Trans. Wireless Commun.*, vol. 19, no. 5, pp. 3376–3389, May 2020.
[16] C. Briso-Rodriguez, J. M. Cruz, and J. I. Alonso, "Measurements and modeling of distributed antenna systems in railway tunnels," *IEEE Trans. Veh. Technol.*, vol. 56, no. 5, pp. 2870–2879, Sep. 2007.
[17] K. Guan, Z. Zhong, J. I. Alonso, and C. Briso-Rodriguez, "Measurement of distributed antenna systems at 2.4 GHz in a realistic subway tunnel environment," *IEEE Trans. Veh. Technol.*, vol. 61, no. 2, pp. 834–837, Feb. 2012.
[18] J. H. Zhang, P. Tang, L. Tian, Z. X. Hu, T. Wang, and H. M. Wang, " 6–100 GHz research progress and challenges for fifth generation (5G) and future wireless communication from channel perspective," *Sci. China Inf. Sci.*, vol. 60, no. 8, pp. 1–16, 2017.
[19] M. Shafi, J. Zhang, H. Tataria, A. F. Molisch, S. Sun, T. S. Rappaport, F. Tufvesson, S. Wu, and K. Kitao, "Microwave vs. millimeter-wave propagation channels: Key differences and impact on 5G cellular systems," *IEEE Commun. Mag.*, vol. 56, no. 12, pp. 14–20, Dec. 2018.
[20] B. Ai, K. Guan, Z. Zhong, C. F. Lopez, L. Zhang, C. Briso-Rodriguez, and R. He, "Measurement and analysis of extra propagation loss of tunnel curve," *IEEE Trans. Veh. Technol.*, vol. 65, no. 4, pp. 1847–1858, Apr. 2016.
[21] C.-X. Wang, A. Ghazal, B. Ai, Y. Liu, and P. Fan, "Channel measurements and models for high-speed train communication systems: A survey," *IEEE Commun. Surveys Tuts.*, vol. 18, no. 2, pp. 974–987, 2nd Quart., 2016.
[22] B. Ai, R. He, Z. Zhong, K. Guan, B. Chen, P. Liu, and Y. Li, "Radio wave propagation scene partitioning for high-speed rails," *Int. J. Antennas Propag.*, vol. 2012, pp. 1–7, Sep. 2012.
[23] K. Guan, G. Li, T. Kurner, A. F. Molisch, B. Peng, R. He, B. Hui, J. Kim, and Z. Zhong, "On millimeter wave and THz mobile radio channel for smart rail mobility," *IEEE Trans. Veh. Technol.*, vol. 66, no. 7, pp. 5658–5674, Jul. 2017.
[24] D. He, B. Ai, K. Guan, Z. Zhong, B. Hui, J. Kim, H. Chung, and I. Kim, "Channel measurement, simulation, and analysis for high-speed railway communications in 5G millimeter-wave band," *IEEE Trans. Intell. Transp. Syst.*, vol. 19, no. 10, pp. 3144–3158, Oct. 2018.
[25] H. Wei, Z. Zhong, K. Guan, and B. Ai, "Path loss models in viaduct and plain scenarios of the high-speed railway," in *Proc. 5th Int. ICST Conf. Commun. Netw. China*, 2010, pp. 1–5.
[26] K. Guan, Z. Zhong, B. Ai, and T. Kurner, "Semi-deterministic path-loss modeling for viaduct and cutting scenarios of high-speed railway," *IEEE Antennas Wireless Propag. Lett.*, vol. 12, pp. 789–792, 2013.
[27] R. He, Z. Zhong, B. Ai, L. Xiong, and H. Wei, "A novel path loss model for high-speed railway viaduct scenarios," in *Proc. 7th Int. Conf. Wireless Commun., Netw. Mobile Comput.*, Sep. 2011, pp. 1–4.
[28] F. Luan, Y. Zhang, L. Xiao, C. Zhou, and S. Zhou, "Fading characteristics of wireless channel on high-speed railway in hilly terrain scenario," *Int. J. Antennas Propag.*, vol. 2013, pp. 1–9, 2013.
[29] Y. Zhang, Z. He, W. Zhang, L. Xiao, and S. Zhou, "Measurement-based delay and Doppler characterizations for high-speed railway hilly scenario," *Int. J. Antennas Propag.*, vol. 2014, pp. 1–8, Apr. 2014.
[30] C. Wang, Y. Yang, A. Ghazal, X. Ge, Y. Liu, and Y. Zhang, "Channel measurements and models for high-speed train wireless communication systems in tunnel scenarios: A survey," *Scientia Sinica Informationis*, vol. 47, no. 10, pp. 1316–1333, Oct. 2017.
[31] M. Berbineau, J. Moreno, S. Kharbech, Y. Yan, A. Vizzari, R. Torrego, J. Soler, L. Clavier, R. Kassi, F. Mazzenga, and R. Giuliano, "Emulation of various radio access technologies for zero on site testing in the railway domain—The Emulradio4rail platforms," in *Proc. TRA*, Helsinki, Finland, 2020, pp. 1–10.
[32] B. Allen, "Defining an adaptable communications system for all railways," in *Proc. 13th Int. Workshop Commun. Technol. Vehicles*, Madrid, Spain, 2018, pp. 1–11.
[33] D. He, B. Ai, K. Guan, L. Wang, Z. Zhong, and T. Kurner, "The design and applications of high-performance ray-tracing simulation platform for 5G and beyond wireless communications: A tutorial," *IEEE Commun. Surveys Tuts.*, vol. 21, no. 1, pp. 10–27, 1st Quart., 2019.
[34] C.-X. Wang, J. Huang, H. Wang, X. Gao, X. You, and Y. Hao, "6G wireless channel measurements and models: Trends and challenges," *IEEE Veh. Technol. Mag.*, vol. 15, no. 4, pp. 22–32, Dec. 2020.
[35] C.-X. Wang, J. Bian, J. Sun, W. Zhang, and M. Zhang, "A survey of 5G channel measurements and models," *IEEE Commun. Surveys Tuts.*, vol. 20, no. 4, pp. 3142–3168, 4th Quart., 2018.
[36] K. Guan, B. Peng, D. He, J. M. Eckhardt, S. Rey, B. Ai, Z. Zhong, and T. Kurner, "Channel characterization for intra-wagon communication at 60 and 300 GHz bands," *IEEE Trans. Veh. Technol.*, vol. 68, no. 6, pp. 5193–5207, Jun. 2019.
[37] K. Guan, B. Ai, B. Peng, D. He, G. Li, J. Yang, Z. Zhong, and T. Kürner, "Towards realistic high-speed train channels at 5G millimeter-wave band—Part I: Paradigm, significance analysis, and scenario reconstruction," *IEEE Trans. Veh. Technol.*, vol. 67, no. 10, pp. 9112–9128, Oct. 2018.
[38] K. Guan, B. Ai, B. Peng, D. He, G. Li, J. Yang, Z. Zhong, and T. Kürner, "Towards realistic high-speed train channels at 5G millimeter-wave band—Part II: Case study for paradigm implementation," *IEEE Trans. Veh. Technol.*, vol. 67, no. 10, pp. 9129–9144, Oct. 2018.
[39] D. He, B. Ai, K. Guan, J. M. Garcia-Loygorri, L. Tian, Z. Zhong, and A. Hrovat, "Influence of typical railway objects in a mmWave propagation channel," *IEEE Trans. Veh. Technol.*, vol. 67, no. 4, pp. 2880–2892, Apr. 2018.
[40] M. Patzold, *Mobile Fading Channels: Modelling, Analysis, & Simulation*. Hoboken, NJ, USA: Wiley, 2002.
[41] J. Yang, B. Ai, S. Salous, K. Guan, D. He, G. Shi, and Z. Zhong, "An efficient MIMO channel model for LTE-R network in high-speed train environment," *IEEE Trans. Veh. Technol.*, vol. 68, no. 4, pp. 3189–3200, Apr. 2019.
[42] N. C. Sagias and G. K. Karagiannidis, "Gaussian class multivariate weibull distributions: Theory and applications in fading channels," *IEEE Trans. Inf. Theory*, vol. 51, no. 10, pp. 3608–3619, Oct. 2005.

HAO QIU (Student Member, IEEE) received the B.E. degree from Beijing Jiaotong University, in 2019, where he is currently pursuing the master's degree with the State Key Laboratory of Rail Traffic Control and Safety, School of Electronic and Information Engineering. His current research interests include in the field of measurement and modeling of wireless propagation channels, high-speed railway communications, vehicle-to-x channel characterization, and indoor channel characterization for high-speed short-range systems including future terahertz communication systems.

JUAN MORENO GARCÍA-LOYGORRI (Senior Member, IEEE) currently works as a Rolling Stock Engineer with the Engineering and Research Department, Madrid Metro, where he has led many projects on railway communications and is also focused on research activities. He is also a part-time Professor and a Researcher with the Universidad Politécnica de Madrid. He has been working in railways since 2007, first on high-speed and then in subways. He has participated in many railway-related research projects like Roll2Rail, EmulRadio4Rail, Run2Rail, and Tecrail. He has authored more than 50 articles on railway communications. His research interests include channel measurement and modeling, railway communications systems, condition-based maintenance for railways, and software-defined radio.

KE GUAN (Senior Member, IEEE) received the B.E. and Ph.D. degrees from Beijing Jiaotong University, in 2006 and 2014, respectively.

In 2009, he was a Visiting Scholar with the Universidad Politécnica de Madrid, Spain. From 2011 to 2013, he was a Research Scholar with the Institut für Nachrichtentechnik (IfN), Technische Universität Braunschweig, Germany. From September 2013 to January 2014, he was invited to conduct joint research with the Universidad Politécnica de Madrid, Spain. He is currently a Professor with the State Key Laboratory of Rail Traffic Control and Safety, School of Electronic and Information Engineering, Beijing Jiaotong University. He has authored or coauthored two books and one book chapter, more than 200 journal and conference papers, and four patents. His current research interests include measurement and modeling of wireless propagation channels, high-speed railway communications, vehicle-to-x channel characterization, and indoor channel characterization for high-speed short-range systems including future terahertz communication systems.

Dr. Guan has been awarded a Humboldt Research Fellowship for Postdoctoral Researchers, in 2015. He is the Pole Leader of European Railway Research Network of Excellence (EURNEX). He was a recipient of the 2014 International Union of Radio Science (URSI) Young Scientist Award. His articles received eight best paper awards, including the IEEE Vehicular Technology Society 2019 Neal Shepherd Memorial Best Propagation Paper Award. He is an Editor of IEEE Access, the *IET Microwaves, Antennas, and Propagation*, and *Physical Communication*, and a Guest Editor of the IEEE Transactions on Vehicular Technology and *IEEE Communications Magazine*. He serves as the Publicity Chair for PIMRC 2016, the Publicity Co-Chair for ITST 2018, the Track Co-Chair for EuCNC, the Session Convener for EuCAP from 2015 to 2019, and a TPC Member for many IEEE conferences, such as Globecom, ICC, and VTC. He has been a delegate in 3GPP and a member of the IC1004 and CA15104 initiatives.

DANPING HE (Member, IEEE) received the B.E. degree from the Huazhong University of Science and Technology, in 2008, the M.Sc. degree from the Universite Catholique de Louvain (UCL) and the Politecnico di Torino (PdT), in 2010, and the Ph.D. degree from the Universidad Politécnica de Madrid, in 2014.

In 2012, she was a Visiting Scholar with the Institut National de Recherche en Informatique et en Automatique, France. She worked with Huawei Technologies from 2014 to 2015 as a Research Engineer. From 2016 to 2018, she conducted Postdoctoral Research at Beijing Jiaotong University, where she is currently an Associate Professor. She has authored or coauthored more than 40 articles, three patents, and one IEEE standard. Her current research interests include radio propagation and channel modeling, ray-tracing technologies, and wireless communication algorithm design. Her articles received five Best Paper awards and the 2019 Applied Computational Eletromagnetics Society (ACES)-China Young Scientist Award.

ZIHENG XU is currently pursuing the bachelor's degree and will pursue the master's program with the Lightwave Laboratory and School of Electronic and Information Engineering, Beijing Jiaotong University, in 2020. He used to take part in the program of Modeling of Millimeter Wave Channel, Madrid Metro, then published an IEEE conference paper as second author. His future research interests include in the field of electromagnetic field and microwave technology.

BO AI (Senior Member, IEEE) received the master's and Ph.D. degree from Xidian University, in 2002 and 2004, China, respectively.

He is currently working with Beijing Jiaotong University as a Professor and Advisor of Ph.D. degree students. He is also the Deputy Director of the State Key Laboratory of Rail Traffic Control and Safety. He is an Associate Editor of IEEE Transactions on Consumer Electronics and an Editorial Committee Member of *Journal of Wireless Personal Communications*. He has authored or coauthored six books, 140 scientific research articles, and 26 invention patents in his research area till now. His current interests include the research and applications OFDM techniques, HPA linearization techniques, radio propagation and channel modeling, GSM for railway systems, and LTE for railway systems. He is an IET Fellow. He graduated in 2007 with great honors of Excellent Postdoctoral Research Fellow in Tsinghua University.

MARION BERBINEAU (Member, IEEE) received the Engineer degree in informatics, electronics, automatics from Polytech'Lille former EUDIL, in 1986, and the Ph.D. degree in electronics from the University of Lille, France, in 1989. She has been the Research Director of Université Gustave Eiffel (previously Ifsttar and Inrets) since 2000. She was the Director of the Leost Laboratory from 2000 to 2013, then the Deputy Director of the COSYS Department, from 2013 to 2017. In addition to research activities and supervision of Ph.D. students, she coordinates the Railway Research, Université Gustave Eiffel. She is also the Pole Leader of the Intelligent Mobility pole of Eurnex (European Railway Research Network of Excellence). Her current interests include wireless communications for connected and automatic vehicles (Trains and Cars) (radio propagation, channel characterization, and modeling, MCM, MIMO, ITS-G5, GSM-R, LTE, and 5G NR). She has already participated to a lot of European and national research projects, since 1990. She is currently the PROJECT LEADER of Emulradio4rail project in the framework of Shift2rail IP2 and involved in several other projects (X2RAIL3, X2RAIL4, and X2RAIL5). She is on the Reserve List of the Scientific Council of Shift2rail program.